Spectroscopy of ^{52,53}Sc

S. Bhattacharyya,[1,*] M. Rejmund,[1] A. Navin,[1,†] E. Caurier,[2] F. Nowacki,[2] A. Poves,[3] R. Chapman,[4] D. O'Donnell,[4,‡] M. Gelin,[1]
A. Hodsdon,[4] X. Liang,[4] W. Mittig,[1] G. Mukherjee,[1,*] F. Rejmund,[1] M. Rousseau,[2] P. Roussel-Chomaz,[1]
K.-M. Spohr,[4] and Ch. Theisen[5]

[1]*GANIL, CEA/DSM-CNRS/IN2P3, Bd Henri Becquerel, BP 55027, F-14076 Caen Cedex 5, France*
[2]*IPHC, UMR7178, IN2P3-CNRS et Université Louis Pasteur, BP28, F-67037 Strasbourg, France*
[3]*Departamento de Fisica Teorica and IFT/CSIC, Universidad Autonoma de Madrid, 28049 Madrid, Spain*
[4]*School of Engineering and Science, University of the West of Scotland, Paisley PA1 2BE, Scotland, United Kingdom*
[5]*CEA-Saclay DSM/DAPNIA/SPhN, F-91191 Gif/Yvette Cedex, France*

Excited states of neutron-rich odd-*A* and odd-odd Sc isotopes, populated in deep inelastic multinucleon transfer reactions, induced by a ^{238}U beam on a thin ^{48}Ca target, have been identified. A strong feeding of both yrast and nonyrast states in such a reaction is illustrated using a combination of a large efficiency spectrometer and a γ detector array. The structure of the populated states is interpreted in terms of the role of the valence proton and neutrons and compared to shell model calculations in the full pf shell.

I. INTRODUCTION

Recent experimental studies of nuclei at the extremes of isospin reveal a modification of the nuclear shell structure for nuclei far from stability [1,2]. To understand the shell evolution and the development of new shell/subshell closures for neutron-rich nuclei, it is necessary to track the migration of single-particle orbitals as a function of isospin. The measurement of these single-particle strengths can best be obtained from single-neutron transfer reactions. Because of experimental constraints, this is possible only in certain cases for the most exotic nuclei [3]. Alternatively, the single-particle level ordering can also be obtained from a study of the configuration of the ground and excited states of a chain of isotopes/isotones.

There has been a large effort to study nuclei around the shell closure $N = 28$ to improve the understanding of the various features demonstrated in this region [2]. The appearance of the $N = 32$ subshell closure (corresponding to the gap between $\nu 2p_{3/2}$ and $\nu 2p_{1/2}$) beyond $^{48}_{20}$Ca$_{28}$, was established in ^{52}Ca [4] and ^{56}Cr [5] using measurements following β-decay and in ^{54}Ti [6] combining results from β-decay and prompt γ-ray spectroscopy. On the other hand, the prediction of evolution of a further gap between $\nu 1p_{1/2}$ and $\nu 0f_{5/2}$ orbitals giving rise to a shell closure at $N = 34$ [7] was found to be inconsistent with the experimental results for ^{56}Ti [8] and the study of low-lying states in odd and even neutron-rich calcium isotopes [9]. For isotopes/isotones around $N/Z = 20$ or 28, the coupling of the valence nucleon across a shell is expected to play an important role in the understanding of the low-lying level structure. The recent observation of the

presence of a nonaxial deformation in ^{48}Ar [10] has indicated the significant role of cross-shell excitations around ^{48}Ca. These diverse experimental indications of the changing shell structure of light neutron-rich nuclei as a function of isospin have been accompanied by extensive theoretical efforts to derive the appropriate effective residual shell model interaction to better describe the structure of these nuclei [11]. A new shell model residual interaction, SDPF-U, has been successfully used [3,12] for the neutron-rich region around $N = 28$ below $Z = 20$.

Odd-odd/odd-even nuclei, because of the presence of unpaired nucleons, are sensitive to slight changes in the effective residual interaction and therefore provide a valuable testing ground for large-scale shell model calculations [13]. However, neutron-rich odd-*A* as well as odd-odd nuclei are much less studied because of their relatively complex level structure and the decreasing production cross sections for nuclei with a high N/Z ratio. The odd neutron-rich nuclei just above the closed proton core of Ca provide a probe of excitations involving an odd neutron to either of the $\nu 1p_{3/2}$, $\nu 1p_{1/2}$, and $\nu 0f_{5/2}$ single-particle orbitals in the presence of excitation of the valence proton(s). The presence of a valence proton in Sc offers the possibility of observing members of the multiplet of states arising from the coupling of the valence proton and neutrons whose study can serve as a constraint to the shell model interaction.

Various reaction mechanisms have been explored to populate nuclei toward larger N/Z ratios and probe their single-particle level structure through in-beam γ-ray spectroscopy. Deep inelastic multinucleon transfer reactions using a large acceptance magnetic spectrometer coupled to a γ detector array have been shown to be a powerful tool to identify new neutron-rich nuclei with small cross sections and their deexcitation γ rays [9,10,14]. The present work reports the observation of the deexcitation γ rays from the excited states of odd-even and odd-odd neutron-rich isotopes $^{51-53}$Sc, obtained from in-beam spectroscopy following deep inelastic multinucleon transfer reactions in inverse kinematics using the

---
*Permanent address: VECC, 1/AF Bidhan Nagar, Kolkata 700 064, India.

†navin@ganil.fr

‡Present address: STFC, Daresbury Laboratory, Daresbury, Warrington WA4 4AD, United Kingdom.

VAMOS-EXOGAM setup at GANIL [15]. The excited states of ^{53}Sc are reported here for the first time.

II. EXPERIMENTAL TECHNIQUES AND RESULTS

The present measurements were made using ^{238}U beams from the CSS1 cyclotron of GANIL, at an energy of 1.31 GeV, incident on a 1 mg/cm^2 thick, enriched ^{48}Ca target. The resulting target-like residues, produced in deep inelastic transfer reactions, were detected and identified using the large acceptance spectrometer VAMOS [15]. The optical axis of the spectrometer was placed at an estimated grazing angle of 35° with respect to the beam axis. The focal plane detection system consisted of two position-sensitive drift chambers separated by a distance of 1 m, a secondary electron (timing) detector (SeD), placed between the two drift chambers, and a segmented ionization chamber followed by a 21-element Si wall. The measured x, y, θ, ϕ at the focal plane and the known magnetic field combined with ion optics were utilized to reconstruct the magnetic rigidity ($B\rho$), the scattering angle, and the path length for each fragment, on an event by event basis. The mass (A) and mass over charge (A/Q), used to identify the charge state of the ions, were obtained from the time of flight (distance of ∼7.5 m) and total energy and the reconstructed $B\rho$, respectively. Further details about the experimental setup can be found in Refs. [9] and [15]. The derived mass spectra of the measured Sc isotopes obtained in the present work are shown in Fig. 1. As can be seen from the inset of Fig. 1, extreme neutron-rich Sc isotopes up to ^{55}Sc ($N/Z = 1.619$) were produced and identified at the VAMOS focal plane. The coincident prompt γ rays from the target-like residues were detected using 11 segmented clover detectors of the EXOGAM [16] array (photo peak efficiency ∼9% at 1 MeV) surrounding the target. The angle between the γ ray detected by the segment of the clover detector and the reconstructed velocity of the target-like ions determined from the measurements of VAMOS spectrometer were used to correct for the Doppler effect on an event by event
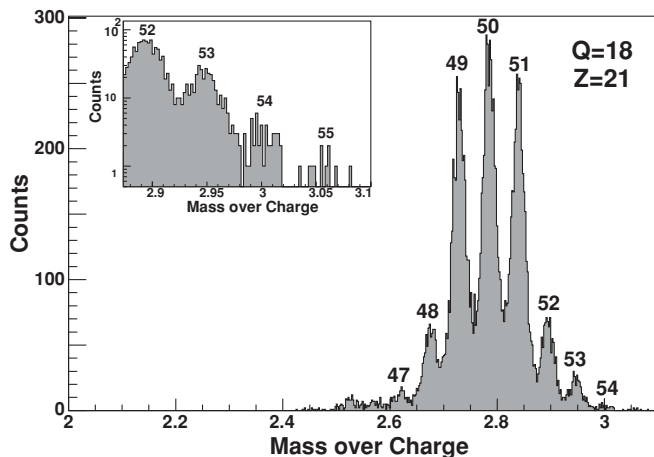

FIG. 1. The reconstructed mass spectrum for a single Si detector in the focal plane for the Sc isotopes and for a selected charge state $Q = 18$. The inset shows the limit of production of the Sc isotopes in a logarithmic scale.
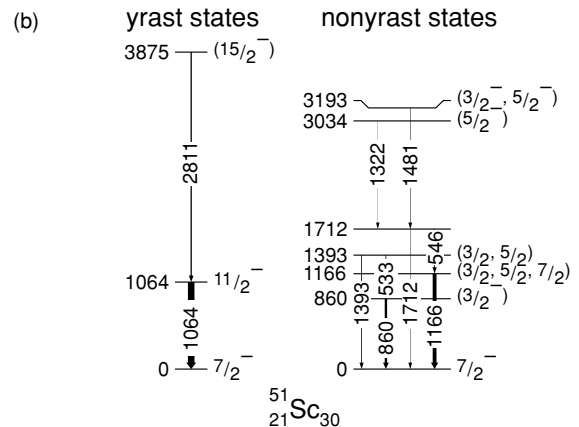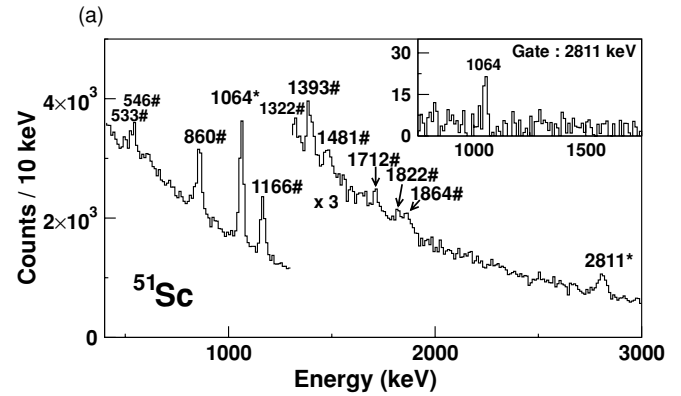

FIG. 2. (a) Doppler corrected γ-ray spectrum for ^{51}Sc; the inset shows the coincidence spectrum for the 2811 keV gate. The γ lines marked as "#" and "∗" correspond to the transitions decaying from nonyrast and yrast states, respectively. (b) The yrast and nonyrast states of ^{51}Sc populated in the present work.

basis. The Doppler corrected γ spectra of ^{51}Sc and ^{52,53}Sc are shown in Fig. 2(a) and Fig. 3, respectively. The corresponding level schemes of ^{51}Sc and ^{52,53}Sc are shown in Figs. 2(b) and Fig. 4, respectively. These level schemes were obtained using the measured γ-γ coincidences and γ-ray relative intensities and were also guided by simple shell model arguments.

A. ^{51}Sc: Yrast and nonyrast states

The results for ^{51}Sc are discussed to illustrate the population of both yrast and nonyrast states in deep inelastic transfer reactions. The initial use of these reactions employed thick targets, stopping the binary reaction fragments within the target material, and the use of high γ-fold coincidence techniques for spectroscopic studies [17]. This method restricts the sensitivity for the population and detection of nonyrast states. In such a method the identification is based on the knowledge of known transitions. On the other hand, identifying directly a nucleus by using a spectrometer has been shown to be an alternate technique [9,10,14]. A rich variety of level structure, both high-spin yrast states and nonyrast excitations, was observed in the above studies, e.g, the strong populations of states linked
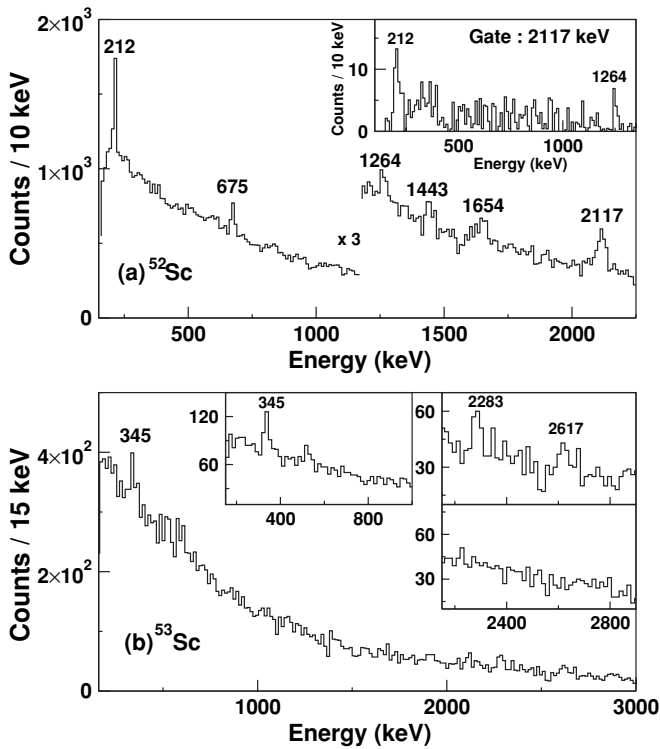
FIG. 3. Doppler corrected γ-ray spectra for (a) ^{52}Sc (the inset shows the coincidence spectrum for the 2117 keV gate) and (b) ^{53}Sc (the inset at the left shows the lower energy part of the spectrum demanding a condition of a higher excitation energy of the fragment, see text). In panel (b), the insets on the right show the expanded view of the higher energy part of the spectrum with (top) and without (bottom) Doppler correction.

with octupole vibration [9,10]. In the case of Sc isotopes, this fact is evident from Figs. 2(a) and 2(b), showing the Doppler corrected γ spectrum and the level structure of ^{51}Sc obtained in the present work. In the β decay of ^{51}Ca ($3/2^-$) to the excited states of ^{51}Sc, feeding to low-lying states with spin $J \leqslant 5/2$ was observed [18]. The most intense γ transitions corresponding to these states have also been observed in the present work and are labeled in Fig. 2 as "nonyrast." Two additional γ rays of 1822(6) and 1864(8) keV have also been observed in the present work, but could not be placed in the level scheme. The other two intense γ transitions of 1064(3) and 2811(8) keV, seen in the spectrum of Fig. 2(a), have been identified as belonging to the yrast cascade of $3875(15/2^-) - 1064(11/2^-) - 0(7/2^-)$ keV on the basis of γ-γ coincidence measurements. The coincidence spectrum corresponding to the gating transition of 2811 keV is shown as an inset in Fig. 2(a). The $3875(15/2^-) - 1064(11/2^-)$ cascade was also reported in a deep inelastic reaction using a thick target [19]. In an earlier study of the three-nucleon transfer reaction ^{48}Ca$(\alpha, p)^{51}$Sc, the 860 keV ($L = 1$, $J^{\pi} = 3/2^-$) and 1064 keV ($L = 5$, $J^{\pi} = 11/2^-$) states were identified [20]. However, the nonyrast γ transitions and the corresponding states, shown in Figs. 2(a) and 2(b), were not observed in Ref. [19]. This illustrates the unbiased observation of various states using a spectrometer for identifying the fragments in deep inelastic multinucleon transfer. Additionally, the large acceptance and efficiency of

the EXOGAM-VAMOS system allows the study of a wide range of isotopes produced under similar conditions allowing the tracking of, for example, octupole excitations.

B. ^{52}Sc

In the odd-odd nucleus ^{52}Sc, four γ-ray transitions, 1264(6), 1443(8), 1654(13), and 2117(8) keV, were identified, in addition to the 675(3) and 212(1) keV transitions observed in the previous β-decay studies [4] and in-beam γ-ray spectroscopy following secondary fragmentation [21]. Following the β-decay study [4], the 675(3) keV transition is placed as decaying from a low-lying 2^+ state to the ground state. The 212(1) keV transition was first observed in Ref. [21] and was proposed to correspond to the 5^+–4^+ decay. The 4^+ state is predicted to be almost degenerate with the 3^+ ground state (the 4^+–3^+ decay was not observed). The 212 keV transition has been also identified in the present work, but the low energy transition corresponding to 4^+ to the ground state (3^+) remains unobserved. Thus it was not possible to determine the exact excitation energy of the first 4^+ state and this is denoted by an "x" in Fig. 4. The 212 keV transition has been found to be in coincidence with two other observed transitions of energies 1264(6) and 2117(8) keV. The coincidence spectrum corresponding to the gating transition of 2117 keV is shown as an inset in Fig. 3(a). On the basis of the intensity balance and the observed coincidences among the 212, 1264, and 2117 keV transitions, these γ rays are placed in cascade, as shown in Fig. 4. The observed new transition of 1443 keV is placed as decaying to the 212 keV level on the basis of energy and intensity balance and thus pointing to a new level at 1654 keV. The presence of this level is also confirmed from the observation of a 1654 keV transition, which has been placed in parallel with the 212–1443 keV cascade. However, no coincidence of the 1443 keV transition with the 212 keV transition could be observed due its weak intensity and lack of statistics in the γ-γ coincidence data. Very recently, independent of the present measurements, the excited states of ^{52}Sc have been reported using deep inelastic reaction [22]. There is an overall agreement between the results (reported here) and those in Ref. [22]. However, the 675, 1443, and 1654 keV transitions and the corresponding excited levels were not observed in Ref. [22]. The population of low-lying nonyrast states along with the yrast transitions, like those observed in ^{51}Sc reported here and in the Ca isotopes [9], thus can also be seen in the present case. The characteristics of these states are further discussed in Sec. III.

C. ^{53}Sc

The transitions in ^{53}Sc are reported here for the first time. Prior to this study, only the half-life and the spin-parity of the ground state were reported [23]. Three new transitions, 345(7), 2283(18), and 2617(20) keV, have been identified in coincidence with the ^{53}Sc fragments detected at the VAMOS focal plane. The corresponding γ spectrum is shown in Fig. 3(b). The presence of the two higher energy peaks was further confirmed from a comparison of the spectra with and
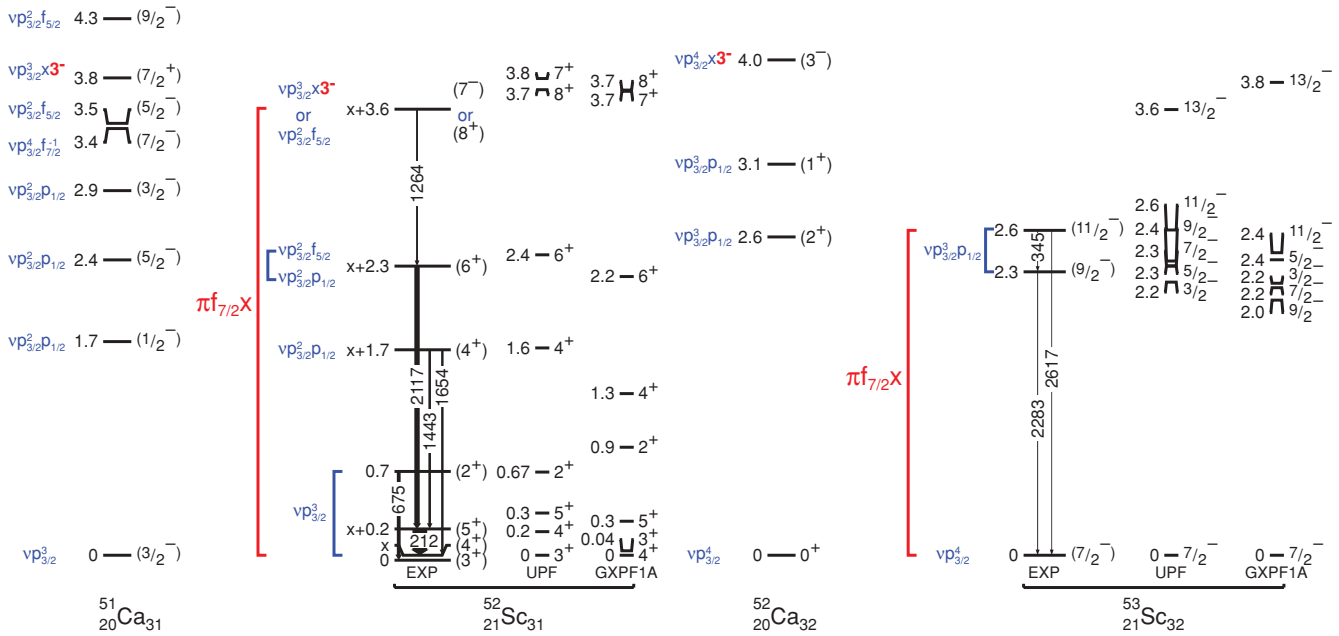
FIG. 4. (Color online) Measured and calculated level schemes for ^{52,53}Sc derived from the present work. The electromagnetic transitions are indicated by arrows; the widths indicate their relative intensities. The theoretical predictions of the shell model calculations using the UPF and GXPF1A effective interactions in the full pf shell valence space are shown as well (see text). The experimental levels of the corresponding isotones in Ca are also shown, which are from Ref. [9], except for the 1^+ state in ^{52}Ca, which is taken from Ref. [24].

without Doppler correction, as shown in the inset in Fig. 3(b). These two transitions are placed in the level scheme shown in Fig. 4 as decaying directly to the ground state. The low-energy transition of 345 keV is tentatively placed in the level scheme as the decaying from the 2283 keV level, on the basis of the energy difference of the two states at 2283(18) and 2617(20) keV. The placement of 345 keV above the 2283 keV transition is further justified by comparing its intensity as a function of excitation energy of the fragment. A γ spectrum corresponding to the higher excitation energy of ^{53}Sc shows a larger yield of 345 keV γ ray, which can be observed from the inset in Fig. 3(b). This method of constraining the excitation energy of the fragment was shown to serve as an additional aid for the placement of γ rays in the case of Ca isotopes produced in the same reaction [9]. It was difficult to observe fragment-γ-γ coincidence with reasonable statistics for this exotic nucleus. The peak-like structures at around 500–600 keV arise due to the ill-corrected Doppler correction of 511 and 596 keV (Ge(n, n')) transitions. The level scheme of ^{53}Sc, shown in Fig. 4, was obtained using energy and intensity balance and guidance from shell model arguments for the possible spin-parity assignments.

III. DISCUSSION

The nature of the states in ^{52,53}Sc, shown in Fig. 4, are first discussed in terms of the coupling of the valence $\pi f_{7/2}$ to the core states in ^{51,52}Ca. Then, they are compared to the results of the interacting shell model calculations. The corresponding levels in ^{51,52}Ca are also shown in Fig. 4. In ^{52}Sc the multiplet of states with $J^\pi = 2^+$–5^+ arise from the coupling of the

$\pi f_{7/2}$ to the ground state $(3/2^-)$ of ^{51}Ca. The 3^+ and 4^+ states are expected to be almost degenerate as discussed in Refs. [21] and [22]. The new level at 1.7 MeV is interpreted to arise from a coupling of a $\pi f_{7/2}$ to the lowest $1/2^-$ state in ^{51}Ca. This could correspond to either a 3^+ state or a 4^+ state. The observation of the $1/2^-$ state in ^{51}Ca was reported [9] from the study of the low-lying states in Ca isotopes. However, both the $1/2^-$ state in ^{51}Ca and the corresponding coupled state at 1.7 MeV in ^{52}Sc was not observed in the work of Ref. [22], probably due to the dominance of yrast cascades, as discussed in Sec. II. The level at 2.3 MeV is likely to correspond to the $5/2^-$ state at 2.4 MeV in ^{51}Ca. The state at 3.6 MeV has been interpreted in Ref. [22] as the 8^+ state analogous to the $9/2^-$ state at 4.3 MeV in ^{51}Ca. However, based on its strong population and that of the $7/2^+$ state in ^{51}Ca (produced in the same reaction [9]), the level at 3.6 MeV could also be interpreted as analogous to the $7/2^+$ state at 3.8 MeV, suggesting it to be a 7^- state. Similarly, the states in ^{53}Sc are expected to reflect a coupling of the valence $\pi f_{7/2}$ to states in ^{52}Ca. The two observed excited states at 2.3 and 2.6 MeV can be associated with the first excited 2^+ state in ^{52}Ca, which leads to a multiplet of states $(3/2^-$–$11/2^-)$.

Shell model calculations have been carried out using the code ANTOINE [25] and the effective interaction UPF [26]. This new pf-shell interaction is the last member of the saga of the Kuo-Brown interactions for the pf shell. It is obtained by means of a fit to 150 low-lying energy levels of nuclei with Z or $N \geqslant 28$ (from ^{48}Ca to ^{64}Ge) using the interaction KB3G [27] as a starting point. For the remaining $0f_{7/2}$ nuclei it gives results equivalent to KB3G. The valence space consists of the full pf shell for protons and neutrons. Negative parity states in ^{52}Sc and positive parity states in ^{53}Sc corresponding

to cross shell excitations cannot be calculated within the above model space.

The results of shell model calculations using the UPF interaction are shown in Fig. 4 and are in good agreement with the experimental values. The shell model interaction, GXPF1A [7], is also widely used for nuclei having their valance nucleons in the pf shell. Calculation of excited states in ^{52,53}Sc using the GXPF1A interaction is also shown in Fig. 4. The observed state at $1654 + x$ keV in ^{52}Sc, populated in the present work, is calculated to be 0.4 MeV lower using the GXPF1A interaction. The corresponding core state in ^{51}Ca is identified as one neutron excitation to the $p_{1/2}$ orbital. A lowering ($\sim$0.5 MeV) of this state in ^{51}Ca, calculated using the GXPF1A interaction, was discussed in Ref. [9]. This has an implication for the energy gap between the $\nu p_{1/2}$ and $\nu f_{5/2}$ orbitals. The shell model configurations for the excited states in ^{52,53}Sc show that they have a dominant contribution from the coupling of the valence $\pi f_{7/2}$ to the states in the neighboring Calcium isotopes as discussed above. These configurations are shown in Fig. 4 and contribute to $\geqslant$70% of the corresponding wave functions in ^{52,53}Sc using both the UPF and GXPF1A interactions. An exception to this is the state at 2.3 MeV in ^{52}Sc. Calculations using the UPF interaction show that the main configurations for this state are 41% from the $\pi f_{7/2} \nu p_{3/2}^2 f_{5/2}$ and 28% from the $\pi f_{7/2} \nu p_{3/2}^2 p_{1/2}$. The shell model calculation with UPF interaction predicts that the parentage of this state arises from two $5/2^-$ states in ^{51}Ca at 3.5 and 2.4 MeV. This large contribution of the high-lying parent state (3.5 MeV in ^{51}Ca) to the observed state at 2.3 MeV in ^{52}Sc is due to the strong interaction (in the model) between the $\pi f_{7/2}$ and $\nu f_{5/2}$ states. However, it is noted that, using the interaction GXPF1A, the dominant configuration for the state at 2.3 MeV is $\pi f_{7/2} \nu p_{3/2}^2 p_{1/2}$ with only 22% admixture of $\pi f_{7/2} \nu p_{3/2}^2 f_{5/2}$. This relates to the fact that the higher lying parent state at

3.5 MeV in ^{51}Ca, which is identified as corresponding to excitation of one neutron to $f_{5/2}$ orbital, is calculated to be high compared with the experimental value [9] using the GXPF1A interaction. Thus the 4^+ state at 1.7 MeV and the 6^+ state at 2.3 MeV in ^{52}Sc have an important connection to the evolution of the energy gap between the $\nu p_{1/2}$ and $\nu f_{5/2}$ states. Similarly, the location of the high spin $13/2^-$ in ^{53}Sc is intimately connected to the $N = 34$ neutron gap.

IV. CONCLUSION

In summary, spectroscopy of the most neutron-rich isotopes of Sc using deep inelastic multinucleon transfer reactions are reported. This work clearly demonstrates the population of both yrast and nonyrast states in deep inelastic transfer reactions and the versatility of using a spectrometer to directly identify the fragments. The levels in these nuclei are interpreted in terms of the coupling of the valence $\pi f_{7/2}$ to states in ^{51,52}Ca and a comparison with shell model calculations confirms the expected domination of this configuration. The study of states involving a single $\pi f_{7/2}$ and a $\nu f_{5/2}$ excitation is very important to constrain the interaction and improve its predictive power. The chain of isotopes of Sc with their unpaired proton provides a good opportunity in this direction. However to populate and pinpoint the relevant key states is an experimental challenge.

[1] J. Dobaczewski, I. Hamamoto, W. Nazarewicz, and J. A. Sheikh, Phys. Rev. Lett. **72**, 981 (1994).

[2] O. Sorlin and M. G. Porquet, Prog. Part. Nucl. Phys. **61**, 602 (2008).

[3] L. Gaudefroy *et al.*, Phys. Rev. Lett. **97**, 092501 (2006); **99**, 099202 (2007); A. Signoracci and B. A. Brown, Phys. Rev. Lett. **99**, 099201 (2007).

[4] A. Huck *et al.*, Phys. Rev. C **31**, 2226 (1985).

[5] J. I. Prisciandaro *et al.*, Phys. Lett. **B510**, 17 (2001).

[6] R. V. F. Janssens *et al.*, Phys. Lett. **B546**, 55 (2002).

[7] M. Honma, T. Otsuka, B. A. Brown, and T. Mizusaki, Phys. Rev. C **69**, 034335 (2004); M. Honma *et al.*, Eur. Phys. J. A **25**, 499 (2005).

[8] S. N. Liddick *et al.*, Phys. Rev. C **70**, 064303 (2004).

[9] M. Rejmund *et al.*, Phys. Rev. C **76**, 021304(R) (2007).

[10] S. Bhattacharyya *et al.*, Phys. Rev. Lett. **101**, 032501 (2008).

[11] E. Caurier *et al.*, Rev. Mod. Phys. **77**, 427 (2005).

[12] F. Nowacki and A. Poves, arXiv:0712.2936 [nuc-th].

[13] A. Novoselsky and M. Vallieres, Phys. Rev. C **57**, R19 (1998).

[14] N. Marginenan *et al.*, Phys. Lett. **B633**, 696 (2006).

[15] S. Pullanhiotan *et al.*, Nucl. Instrum. Methods A **593**, 343 (2008).

[16] J. Simpson *et al.*, Heavy Ion Phys. **11**, 159 (2000).

[17] R. Broda, J. Phys. G: Nucl. Part. Phys. **32**, R151 (2006).

[18] A. Huck *et al.*, Phys. Rev. C **22**, 2544 (1980).

[19] R. Broda *et al.*, Acta Phys. Pol. B **36**, 1343 (2005).

[20] R. O. Ginaven *et al.*, Nucl. Phys. **A154**, 417 (1970).

[21] A. Gade *et al.*, Phys. Rev. C **73**, 037309 (2006).

[22] B. Fornal *et al.*, Phys. Rev. C **77**, 014304 (2008).

[23] O. Sorlin *et al.*, Nucl. Phys. **A632**, 205 (1998).

[24] F. Perrot *et al.*, Phys. Rev. C **74**, 014313 (2006).

[25] E. Caurier and F. Nowacki, Acta Phys. Pol. B **30**, 705 (1999).

[26] E. Caurier, F. Nowacki, and A. Poves, Phys. Rev. C (in press).

[27] A. Poves, J. Sanchez Solano, E. Caurier, and F. Nowacki, Nucl. Phys. **A694**, 157 (2001).